Harmonic analysis of high penetration level of Photovoltaic generation in distribution network and solution studies

Citation for published version:
Xiong, L, Nour, MI & Shahin, M 2019, Harmonic analysis of high penetration level of Photovoltaic generation in distribution network and solution studies. in *8th International Conference on Modeling Simulation and Applied Optimization (ICMSAO).*, 8880387, IEEE, 8th International Conference on Modeling Simulation and Applied Optimization 2019, Manama, Bahrain, 15/04/19. https://doi.org/10.1109/ICMSAO.2019.8880387

Digital Object Identifier (DOI):
10.1109/ICMSAO.2019.8880387

Link:
Link to publication record in Heriot-Watt Research Portal

Document Version:
Peer reviewed version

Published In:
8th International Conference on Modeling Simulation and Applied Optimization (ICMSAO)

Harmonic analysis of high penetration level of Photovoltaic generation in distribution network and solution studies

Lue Xiong
School of Engineering and Physical Sciences
Heriot-Watt University Dubai
Dubai, UAE
lx9@hw.ac.uk

Mutasim Nour
School of Engineering and Physical Sciences
Heriot-Watt University Dubai
Dubai, UAE
mutasim.nour@hw.ac.uk

Moustafa Shahin
School of Engineering and Physical Sciences
Heriot-Watt University Dubai
Dubai, UAE
ms179@hw.ac.uk

***Abstract*—The high penetration level of Photovoltaic (PV) generation in distribution network reduces carbon emissions but also becomes problematic in terms of network management. Harmonic distortion is the main factor studied in this paper and a typical three-bus distribution network is built in MATLAB/Simulink to understand the harmonics problem. Results show that current harmonics are more vulnerable to fluctuate compared to voltage harmonics. Based on existing harmonic standards, total demand distortion of current (TDD_i) is evaluated to estimate maximum PV penetration level at Point of Common Coupling (PCC), and the maximum acceptable TDD_i at each bus differs according to specific loading and short-circuit levels. Meanwhile, total harmonic distortion of current (THD_i) at inverter outputs represents inverter performance. Instead of assessing at standard test conditions (STC), the impact of irradiance variations is studied. Low irradiance results in an increased THD_i of the inverter whilst doesn't explicitly affect TDD_i at PCC. A simple and low-cost solution is proposed to dynamically vary the settings of inverter's filter elements against irradiance, and harmonic distortion at low irradiance of the inverter is successfully mitigated.**

Keywords—total harmonic distortion, total demand distortion, irradiance, PV penetration level, power system

I. INTRODUCTION

Photovoltaic (PV) generation is one widely applied form of Renewable Energy Generation (REG), which turns universally available solar energy into electricity through photovoltaic effect [1]. Unlike fossil fuels, the intermittent and non-dispatchable nature of REG pose new threats to power systems, and potential impacts include voltage fluctuations, harmonics, reverse power flows and malfunction of protection devices [2]. Meanwhile, the PV generation can be either connected to transmission or distribution network, and the severity of corresponding problems also varies.

Inverter which transforms energy forms from DC to AC is a basic element in PV system. However, the conversion process can inject undesired harmonics at lower order into power system [3]. Excessive harmonic voltage and current induce extra losses like core losses in transformers and generators, as well as increase transmission losses in conductors, which further cause overheating and affect lifecycles of power equipment and potentially result in maloperation of protective devices [4]. Most inverter datasheets specify the maximum distortion limit at rated output conditions. For instance, SUN2000-8/12KTL manufactured by HUAWEI sets the maximum distortion limit to 3% [5]. Obviously, solar inverters cannot always work under rated conditions, the validity of this harmonic limit under irradiance variations hasn't been addressed.

The commonly used indicator to reflect the distortion levels is Total Harmonic Distortion (THD) which is the ratio of the rms magnitude of the harmonics (excluding fundamental) to the fundamental rms value [6]. THD expression for current is given by:

$$\mathrm{THD}_i = \sqrt{\sum_{n=2}^{\infty} I_n^2} \Big/ I_1 \tag{1}$$

Where I_1 is the rms fundamental current, I_n is the rms value of current at n^{th} harmonics. Same formula applies to THD expression for voltage.

Various standards such as IEEE 919, IEEE 519-2014, IEC 61000, IEC 61727 and EN 50160 are proposed by industry to regulate harmonic injections within proper levels. Instead of using fixed harmonic distortion limits, IEEE standards set harmonic constraints based on voltage levels and the ratio of maximum short-circuit current (I_{sc}) to maximum demand current (I_L). Specifically, current distortion limits are presented in Table I, which vary under different I_{sc}/I_L [7].

TABLE I. MAXIMUM HARMONIC CURRENT DISTORTION IN PERCENT OF I_L INDIVIDUAL HARMONIC ORDER (ODD HARMONICS)

I_{sc}/I_L	<11	11≤h<17	17≤h<23	23≤h<35	23≤h≤50	TDD
<20	4.0	2.0	1.5	0.6	0.3	5.0
20<50	7.0	3.5	2.5	1.0	0.5	8.0
50<100	10.0	4.5	4.0	1.5	0.7	12.0
100<1000	12.0	5.5	5.0	2.0	1.0	15.0
>1000	15.0	7.0	6.0	2.5	1.4	20.0

The application of I_{sc}/I_L ratio is a good representation of relative importance of the studied target on power system in terms of harmonic injection [8]. Specifically, a higher I_{sc}/I_L value indicates that demand current is insignificant compared to the network size, thus a high distortion limit is allowed since this impact is minimal. As described in (2), Total Demand Distortion (TDD) mentioned in Table I is the ratio of the square root of the total squared harmonic current components to the maximum load current.

$$\mathrm{TDD}_i = \sqrt{\sum_{n=2}^{\infty} I_n^2} \Big/ I_L \tag{2}$$

Where I_n is the rms value of current at n^{th} harmonics, and I_L is the maximum load current.

Many researchers have simulated harmonic scenarios against irradiance variations either using software tools or field-testing results. In [9], PQ analyzer is used in the 1.22MW rooftop PV system in University of Queensland for harmonic measurements. Results show that THD_v is within IEEE standards during the day and reaches to maximum at peak solar generation (1.4%). In contrast, THD_i is inversely proportional with solar irradiance since the fundamental current is less during early morning and late afternoon. Similarly, based on detailed inverter models, authors in [10] found that THD_i increases at lower irradiance compared to Standard Test Condition (STC) of 1000W/m^2 whilst THD_v maintains the same. However, differences between THD_i and TDD_i haven't been identified and discussed in abovementioned papers.

To mitigate harmonic problems, adding extra filters and modifying inverter controllers are two commonly proposed solutions. In [11], the combination of a notch filter and a high-pass filter is added in parallel with existing capacitors to reduce both THD_v and THD_i. A hybrid proportional-resonant (PR) controller and repetitive controller is designed in [12] to address THD_i issues with specially tuned parameters. However, PR controller performs well only for single-phase inverter, which limits its application range. Instead of adding extra complexities into inverter designs, a simple and cost-saving method is proposed in this paper and tested at different operating conditions like irradiance variations are also covered.

To quantify the maximum PV capacity that the distribution network can sustain, the PV penetration factor (PVPF) is introduced as the ratio of the aggregated PV capacity in specified area to the rating of distribution transformer which provides local services [13]. Its formula is given by (3). The maximum PVPF is limited by either voltage or current harmonic constraints mentioned in IEEE std 519-2014.

$$PVPF = \left(C_{PV} / S_{TF}\right) \times 100\% \tag{3}$$

Where C_{PV} is the aggregated PV capacity within specified area (kWh); S_{TF} is rating of distribution transformer (kVA).

The aim of this paper is to investigate maximum PV penetration level and its effects on the acceptable harmonic standards. Matlab/Simulink is used to simulate the harmonic problem caused by PV penetration within a typical distribution network, incorporating scenarios like irradiance variations. Also a simple and low-cost measure is proposed and implemented to mitigate the harmonic problem.

II. Methodology

A. PV penetration in three-bus distribution network

In Fig.1, a typical 25kV/60Hz distribution network in North American is used, and three buses are connected radially [14]. The whole system is implemented in Matlab/Simulink.

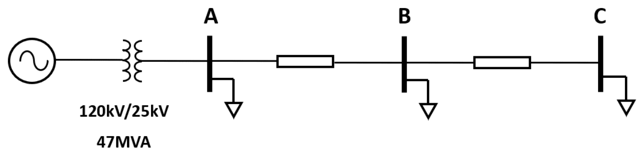

Fig. 1. Single line diagram of three-bus distribution network

Load information is presented in Table II, which is modified from the original network.

TABLE II. LOAD DETAILS FOR THREE-BUS NETWORK

Bus	Active P	Reactive Q	Power Factor
A	30MW	2MVAr	0.99
B	2MW	0	1
C	250kW	0	1

With reference to [14], a 250kW PV system is designed and its generic diagram is shown in Fig.2. The key components are introduced separately.

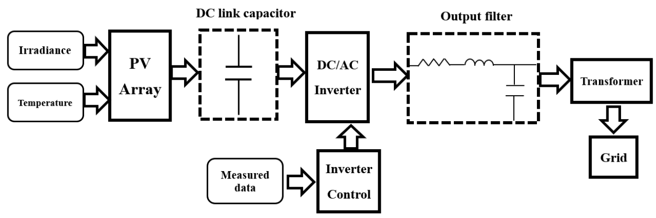

Fig. 2. Single line diagram of three-bus distribution network

To obtain PV capacity of 250kW, the industry-verified PV panel (SunPower SPR-415E-WHT-D) is selected with 415W as DC capacity. 88 panels are parallel-connected with 7 panels connected in series. The three-level based IGBT bridge circuit is implemented for DC/AC conversion. The converter is pulse width modulated (PWM), which is used in the inverter control block.

DC link capacitor is required to compensate 120 Hz power ripple on the DC bus caused by the AC load side of the inverter [15]. The required capacitance to buffer the ripple is based on the output power during 1/8th fundamental cycle, which is given in [15]:

$$\begin{aligned} P_{ac} &= \Delta E/(T/8) = (1/2)\left[CV^2 - C(V-\Delta V)^2\right] \times 8 f_{ac} \\ C_{link} &= \left(P_{ac}/4 f_{ac}\right) \times \left[1/\left(2V\Delta V - \Delta V^2\right)\right] = \left(P_{ac}/4 f_{ac}\right) \times \left(1/2V\Delta V\right) \end{aligned} \tag{4}$$

Where, P_{ac} is rated output power in kW from AC side - 250kW, f_{ac} is 60Hz, V is DC voltage decided by PV array - 480V for 7 panels in series, ΔV is the specified maximum voltage ripple, also power ripple.

In (4), ΔV^2 is regarded as minimal which can be neglected. Assume power ripple (ΔV) of 40V is acceptable, so the value of required capacitance is calculated as:

$$C_{link} = \left[250 \times 10^3 / (4 \times 60)\right] \times \left(1/2 \times 480 \times 40\right) = 0.0271F \tag{5}$$

The output filter is mainly designed for smoothing out harmonics. A series RL choke circuit and a C-filter in parallel. The RL choke, also known as line reactor is designed to attenuate harmonics and protect equipment against transient overshoots [16]. The inductance dominants in the choke circuit, and (6) shows calculation process [17].

$$\begin{aligned} L_{choke} &= k \times \left(1/2\pi f_{ac}\right) \times \left(V_{L-L}/\sqrt{3}\, I_{rms}\right) = kV_{L-L}^2 / 2\pi f_{ac} P_{ac} \\ &= \left(0.15 \times 250^2\right) / \left(2\pi \times 60 \times 250 \times 10^3\right) = 9.95 \times 10^{-5} H \end{aligned} \tag{6}$$

Where V_{L-L} is the line voltage at the inverter output (250V) obtained from DC link voltage, I_{rms} is rms current flowing through choke inductor, k value is 0.15 by default.

The C-type filter is used for reducing harmonics and improving reactive power. A small capacitor is designed with its rated reactive power 10% of rated PV output.

B. Adaptive inverter filter settings

Instead of altering inverter control logic or adding a separate well-tuned filter, a simple method which changes settings of passive filter elements is presented. Already shown in (4) and (6), parameters like f_{ac}, V and V_{L-L} have less fluctuations because of grid connection and inverter control logics, which can be regarded as constants. Since active power P_{ac} is directly proportional to irradiance, the relationship between passive elements and irradiance is given in (7) and (8).

$$C_{link} = (P_{ac}/4f_{ac}) \times (1/2V\Delta V) \propto P_{ac} \propto I_{irradiance} \quad (7)$$

$$L_{choke} = kV_{L-L}^2 / 2\pi f_{ac} P_{ac} \propto 1/P_{ac} \propto I_{irradiance} \quad (8)$$

Where $I_{irradiance}$ is the irradiance level in W/m^2.

Results above indicate that best-fit filter parameters under different irradiance levels should not be constants at rated outputs. Table III lists the optimal filter parameters under the different irradiance levels with a gap of $200W/m^2$. The feasibility of the proposed adaptive settings is studied through simulation in the following sections.

TABLE III. CALCULATED FILTER PARAMETERS FOR DIFFERENT IRRADIANCE

Irradiance (W/m^2)	1000	800	600	400	200
C_link (F)	0.0543	0.04344	0.03258	0.02172	0.01086
L_choke (H)	9.95E-05	1.24E-04	1.66E-04	2.49E-04	4.98E-04

III. SIMULATING HARMONIC PROBLEM IN THREE-BUS POWER SYSTEM

In the three-bus distribution network model in Fig.1, the I_{sc}/I_L of each bus is evaluated. I_L is measured as steady-state current flow, whilst I_{sc} is obtained by applying a balanced three-phase fault on each bus. Allowable current harmonics (expressed as TDD_i) for each bus are obtained with reference to IEEE std. 519 [8]. Results are shown in Table IV:

TABLE IV. HARMONIC LIMITS FOR EACH BUS

Bus	A	B	C
I_{sc}/I_L	8.3	34.3	222
Max. TDD_i	5%	8%	15%
Max. THD_v	5%	5%	5%

A. Base case for 250kW at bus C

Based on Fig.1 and Fig.2, the 250-kW PV system is initially connected to bus C, so bus C is the PCC between PV and load. PVPF for this case is evaluated as:

$$PVPF = (C_{PV}/S_{TF}) \times 100\% = 250kW/47MVA \times 100\% = 0.53\% \quad (9)$$

THD_v and THD_i for each bus under different irradiance levels are measured and presented in Table V and Table VI. Compared to THD_i, THD_v at all buses are negligible under this level of PV penetration. Meanwhile, without any voltage compensation devices, the harmonic level decreases from bus C to bus A at the source.

TABLE V. THD_V AT EACH BUS FOR PV AT BUS C

Irrdiance level (W/m^2)	BusA	BusB	BusC
1000	0.01%	0.07%	0.11%
800	0.01%	0.07%	0.10%
600	0.01%	0.07%	0.10%
400	0.01%	0.07%	0.11%
200	0.01%	0.07%	0.10%

TABLE VI. THD_I AT EACH BUS FOR PV AT BUS C

Irrdiance level (W/m^2)	BusA	BusB	BusC	Bus PV
1000	0.01%	0.18%	37.95%	1.61%
800	0.01%	0.14%	5.33%	1.67%
600	0.01%	0.14%	2.84%	2.20%
400	0%	0.14%	2.03%	3.49%
200	0%	0.13%	1.48%	6.97%

The relationship between THD_i and TDD_i is described in (10). Both THD_i and TDD_i at bus C are evaluated and shown in Table VII.

$$THD_i \times I_1 = TDD_i \times I_L \quad (10)$$

TABLE VII. THD_I AND TDD_I AT BUS C

Irrdiance level (W/m^2)	THDi	I_1(A)	I_L(A)	TDDi
1000	37.95%	0.323	5.7	2.15%
800	5.33%	1.885	5.7	1.76%
600	2.84%	3.465	5.7	1.73%
400	2.03%	5.051	5.7	1.80%
200	1.48%	6.644	5.7	1.73%

In Table VII, THD_i at $1000W/m^2$ is extremely high due to low fundamental current I_1. However, according to IEEE std 519-2014, TDD_i is a true reflection for harmonic distortion at PCC. In this case, TDD_i is around 2% under different irradiance, which is within the 15% limit specified in Table IV.

B. Investigating penetration limit

To identify allowable penetration limits at each bus, a series of simulation is performed for the PV array of different sizes individually connected to each bus. Assumptions include:

- The size of PV array increases from 500kW with a step size of 500kW (equivalent to 1% PVPF for this radial network);
- Harmonic levels are assessed at two irradiance levels: $1000W/m^2$ and $200W/m^2$, which represent cases of standard irradiance and low irradiance;
- Simulation stops when any of three criteria (THD_v, TDD_i and individual harmonic levels in Table I) reaches the harmonic limit of this bus at any irradiance level ($1000W/m^2$ or $200W/m^2$).

THD_v against increasing PV penetration at bus C is shown in Fig. 3. A positive linear relationship is observed between voltage distortion and PV penetration capacity. THD_v under both is well below specified 5% limit.

TDD_i against increasing PV penetration at bus C is presented in Fig. 4. In comparison, current distortion at PCC is more significant under standard irradiance compared to low irradiance. The maximum allowable PV capacity at bus C is 1,800kW, which accounts for 3.8% of PVPF.

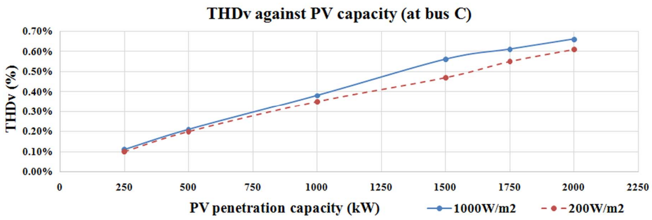

Fig. 3. THD_v against PV capacity (at bus C)

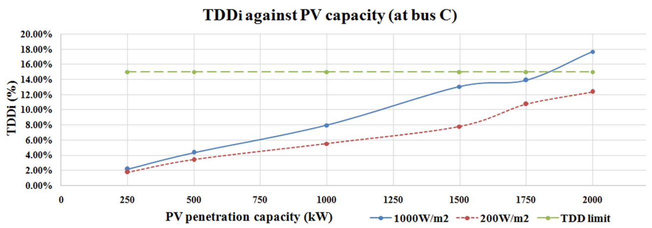

Fig. 4. TDD_i against PV capacity (at bus C)

Similarly, maximum penetration levels at bus A and bus B are investigated and summarized in Table VIII. TDD_i is the dominant factor determining PVPF, and the impact of THD_v is negligible. Results of PVPF show that the bus nearer to the grid can accommodate more PV panels. However, if ratio of PV capacity to local load is considered, the far-end bus can withstand a higher degree of PV penetration. Therefore, case-by-case examination is required for the penetration assessment.

TABLE VIII. SUMMARY FOR PV PENETRATION INVESTIGATION

Bus	Max. PVPF	Max. PV level (MW)	Max. load (MW)	PV/load ratio
A	40.4%	19	30	0.6
B	18.1%	9	2	4.5
C	3.8%	1.8	0.25	7.2

C. *Investigating irradiance impact*

To study the impact of irradiance on current distortion at PCC, the same 1,000kW PV array is connected individually to all buses, and TDD_i of all buses under varying irradiance is illustrated in Fig. 5.

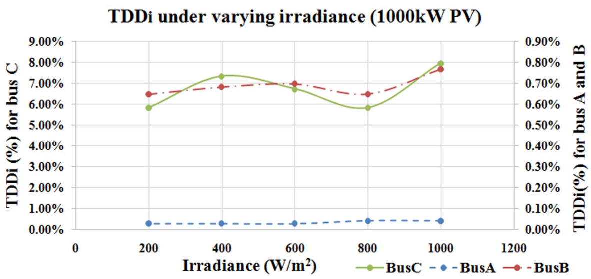

Fig. 5. TDD_i under varying irradiance with 1000kW PV at each bus

IV. ADAPTIVE FILTER SETTING TO MITIGATE HARMONICS

Previous section shows that application of IEEE std 519-2014 at PCC and current distortion is assessed by TDD_i, which describes the interaction between PV and load at PCC. However, to assess the power quality from inverter alone, the THD_i directly at inverter output should be used. For instance, the last column in Table VI is plotted in Fig. 6 for illustration.

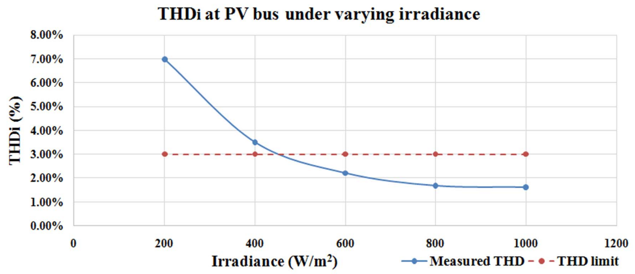

Fig. 6. THD_i at PV bus under varying irradiance (base case)

Fig. 6 shows that the harmonic level at inverter output is inversely related to the irradiance. The 3% distortion limit is breached for the irradiance less than 400W/m^2.

Having discussed in the methodology part, optimal filter settings vary under certain irradiance levels is presented in Table III. Using the base case of 250kW PV, simulation is performed to compare cases of nominal settings at STC and adaptive settings. Results are illustrated in Fig. 7.

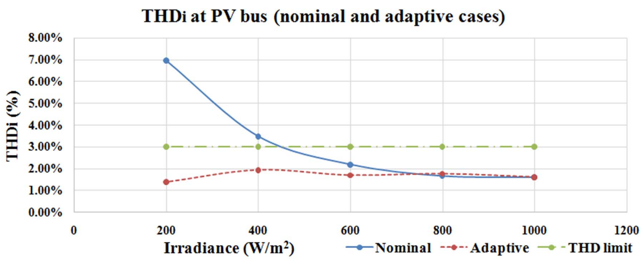

Fig. 7. THD_i at PV bus (nominal and adaptive cases)

Results show that the proposed adaptive method effectively attenuates harmonics within specified limits, which outperforms the fixed nominal settings.

The concept of adaptive settings is like potentiometer, which slides or rotates to proper position to get desired values of passive elements. The control signal can either come from external sensors which measures irradiance or internal lookup table that stores historical irradiance records. In this example, five categories are specified for classifying the input irradiance, and each category corresponds to one group of filter settings. Fig. 8 shows generic control logic.

The number of classification groups in Fig. 8 depends on actual application. More group number means more accurate control but increased switch operations which may reduce equipment lifecycles. Overall, the proposed algorithm is cost-effective since only series inductor is required to increase, and capacitance remains the same when compared to nominal settings.

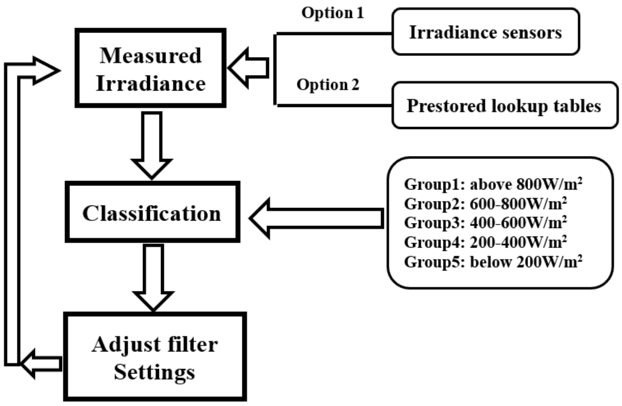

Fig. 8. Generic control logic of adaptive inverter settings

V. Discussions

Unlike stable voltage profiles, more stochastic factors are imbedded within current profiles, and optimal power balancing is always problematic for network operators. This situation deteriorates under high level PV penetration since distribution network is no longer passive and reverse power flow becomes possible. Three common confusions are clarified in this paper: firstly, current harmonics at PCC should be assessed by TDD_i, which measures harmonics after the combination of PV and load. Therefore, the load of a larger size can generally accommodate more PV penetration. Meanwhile, the harmonic distortion of inverters should be measured by THD_i directly at inverter's output, which is independent of load variations. Secondly, since irradiance intensity can vary from zero to $1000W/m^2$ within one day, the impact of irradiance on harmonics should be seriously considered. However, based on investigations so far, existing researchers haven't covered this aspect. Simulation results show that THD_i of inverter under low irradiance can cause harmonic level above the objective limit of 3% specified in simulation, which should be mitigated by manufacturers. In contrast, though the relationship between TDD_i at PCC and irradiance is not explicit, the TDD_i at $1000W/m^2$ represents the highest harmonic values under all irradiance levels. Thirdly, the standard current distortion should not be a fixed limit, I_{sc}/I_L ratio should be measured, which indicates the relative importance of load bus on the overall distribution network. All these factors further urge the need to develop an adaptive solution varying filter parameter to mitigate harmonics.

VI. Conclusions

The impact of high PV penetration level on harmonics is studied in this paper. The difference between THD and TDD about current distortion is distinguished. Based on the typical distribution network model built in Simulink, results of TDD_i at PCC between PV and load are measured and the PV penetration level positively contributes to the TDD_i increase. Meanwhile, TDD_i limits on each bus are different because of I_{sc}/I_L ratio. More harmonic distortion in percent is allowed when load is insignificant to the grid. The maximum allowable PV capacity at each bus is evaluated, and the bus nearer to external grid can accommodate more. Furthermore, the impact of irradiance variations on TDD_i is minimal, and the TDD_i under standard irradiance of $1000W/m^2$ can represent the worst scenario. However, low irradiance affects THD_i at inverter output, which should be mitigated by improving the inverter design. A simple and cost-effective solution is proposed and tested, through adaptive adjustment of passive filter elements with respect to irradiance levels. Reduced harmonics are observed from simulation results. Theoretical analysis and software simulation are principal methodologies applied in this paper, and practical experiments are to be implemented in the next stage.

Acknowledgment

We would like to offer special thanks to Heriot-Watt University Dubai Campus, for its advanced research resources and facilities.

References

[1] Luque, A. and Hegedus, S. (2011) Handbook of photovoltaic science and engineering / edited by Antonio Luque and Steven Hegedus, 2nd ed. ed., Hoboken, N.J. : Chichester: Hoboken, N.J. : Wiley ; Chichester : John Wiley distributor.

[2] Karimi, M., Mokhlis, H., Naidu, K., Uddin, S. and Bakar, A. H. A. (2016) 'Photovoltaic penetration issues and impacts in distribution network – A review', *Renewable and Sustainable Energy Reviews*, 53, 594-605.

[3] Moeed Amjad, A. and Salam, Z. (2014) 'A review of soft computing methods for harmonics elimination PWM for inverters in renewable energy conversion systems', *Renewable and Sustainable Energy Reviews*, 33, 141-153.

[4] Martin, D., Goodwin, S., Krause, O., et al. (2014): 'The effect of PV on transformer ageing: University of Queensland's experience'. *Australasian Universities Power Engineering Conf.*, pp. 1–6.

[5] HUAWEI (2018) *'Smart String Inverter (SUN2000-8/12KTL)'*, [Online], Available: solar.huawei.com/en-eu/commercial/3.pdf [Accessed 6th Feb 2018].

[6] Erickson, R. W. (2001) Fundamentals of power electronics / Robert W. Erickson, Dragan Maksimović, 2nd ed. ed., Boston, Mass. ; [Great Britain]: Boston, Mass. ; Great Britain : Kluwer Academic Publishers.

[7] IEEE Recommended Practice and Requirements for Harmonic Control in Electric Power Systems," in IEEE Std 519-2014 (Revision of IEEE Std 519-1992) , pp.1-29, 11 June 2014.

[8] T. M. Blooming and D. J. Carnovale, "Application of IEEE STD 519-1992 Harmonic Limits," *Conference Record of 2006 Annual Pulp and Paper Industry Technical Conference*, Appleton, WI, 2006, pp. 1-9.

[9] Chidurala, A., Saha, T. K. and Mithulananthan, N. (2016) 'Harmonic impact of high penetration photovoltaic system on unbalanced distribution networks – learning from an urban photovoltaic network', *IET Renewable Power Generation*, 10(4), 485-494.

[10] R. O. Anurangi, A. S. Rodrigo and U. Jayatunga (2017), "Effects of high levels of harmonic penetration in distribution networks with photovoltaic inverters," *2017 IEEE International Conference on Industrial and Information Systems (ICIIS)*, pp. 1-6.

[11] Dartawan, K., Austria, R., Hui, L. and Suehiro, M. (2012) 'Harmonics issues that limit solar photovoltaic generation on distribution circuit', *SOLAR 2012, World Renewable Energy Forum (WREF 2012)*, pp.1-7.

[12] Yang, Y., Zhou, K. and Blaabjerg, F. (2016) 'Current Harmonics From Single-Phase Grid-Connected Inverters—Examination and Suppression', *IEEE Journal of Emerging and Selected Topics in Power Electronics*, 4(1), 221-233.

[13] A. Latheef, D. A. Robinson, Gosbell, V. J. and Smith, V. W. (2006) 'Harmonic impact of photovoltaic inverters on low voltage distribution systems', *in Conference Proceedings of the 2006 Australasian Universities Power Engineering Conference*, pp. 1-6.

[14] MathWorks (2018) *'250-kW Grid-Connected PV Array'*, [Online], Available: https://goo.gl/2PjqZh [Accessed 1st July 2018].

[15] Bhardwaj, M. and Subharmanya, B. (2013) 'PV Inverter Design Using Solar Explorer Kit', *Texas Instruments Incorporated*, pp.19-20.

[16] Kalair, A., Abas, N., Kalair, A. R., Saleem, Z. and Khan, N. (2017) 'Review of harmonic analysis, modeling and mitigation techniques', *Renewable and Sustainable Energy Reviews,* 78, 1152-1187.

[17] MTECorp (2012) *'RL Line Load Reactors'*, [Online], Available: https://goo.gl/b5itHd [Accessed 1st July 2018].